Pulsed electrode deposition of superhard coatings on steel substrates: microstructural and chemical study

M. E. Constantino[1], B. Campillo*[2,3], M. H. Staia[4], S. Serna[1], J. Juárez-Islas[5] and T. S. Sudarshan[6]

Titanium carbide (TiC) coatings have been deposited on steel using the pulsed electrode deposition (PES) technique. Different experimental parametric conditions were used in the deposition process. Microstructural and chemical characterisations of the coatings were performed using electron microscopy and X-ray diffraction techniques. Pulsed electrode technique produced hard coatings, which are commonly defect and crack free. Small TiC and Fe_3C particles were randomly distributed in a Fe matrix without any preferred crystallographic orientation. The relationships between the microstructural properties and the deposition processing conditions were also explored.

Keywords: Pulsed electrode, Titanium carbide, Morphologies, Topographical characteristics

Introduction

The modifications by surface engineering of materials lead to improved properties such as corrosion resistance, wear resistance, hardness and high temperature strength. Hard coatings are commonly used in a wide range of engineering applications because of their high hardness, and good wear and corrosion resistance. The use of ceramic and metal coatings is often a possible approach to increase service life of engineering components. Therefore, for example, the cutting rates of machining processes can be increased by the use of hard metals and ceramics. Titanium carbide (TiC) is a hard compound with physical properties such as high hardness, high melting temperature and high electrical conductivity. These properties make this compound very convenient for use as a protective coating against wear and also corrosion.[1,2] Different surface modification processes, which include physical vapour deposition (PVD), chemical vapour deposition (CVD),[3–6] spray coating,[7] sputtering,[8,9] laser surface engineering (LSE)[10,11] and pulsed electrode deposition (PES),[11,12] are commonly used to deposit hard coatings. Some of these techniques are limited in scope owing to factors, such as the cost of a vacuum chamber, poor bond strength and size of the workpiece. Among all the techniques, PES offers some advantages over the other methods. For example, it has the ability to apply metallurgically bonded coatings with low temperature during the deposition process and also with the absence of toxic or explosive gases. Pulsed electrode deposition is a microwelding process, which uses very short duration, high current electrical pulses to deposit electrode material on a metallic substrate. The low heat input during the process allows the bulk substrate material to remain at or near ambient temperature. This minimises the thermal distortions and also the changes in the metallurgical structure of the substrate. The obtained coating is metallurgically bonded, therefore, it is inherently more resistant to damage and spalling than the mechanically bonded coating produced with other low heat input processes, such as detonation gun, plasma spray, electrochemical plating, etc.[13] Pulsed electrode deposition coatings are used for several applications such as industrial cutting tools, high temperature sensors[14] and turbine coatings for aerospace applications,[15] geothermal and nuclear environments[13] and for wear resistant surfaces on large agricultural and textile equipment.[13,16,17] Pulsed electrode deposition surface engineering has demonstrated the capability of reducing downtime by increasing functional longevity of tools, equipment and components. Agarwal *et al.*[12] have studied TiC coatings on AISI 1018 steel substrate deposited using PES with a current of 25 A. They reported the existence of a metallurgical bond between the coating and the substrate, an irregular morphology of the coating and also a high value of hardness. It has also been recognised in the past[18–20] that the coating physical properties are not only strongly dependent on the materials employed in the deposition process and its stoichiometry but also on the structural characteristics of the coated layer and therefore on the deposition parameters.[20,21] In this investigation, chemical and microstructural characterisations of a TiC coated layer deposited on steel

[1]CIICAP, UAEM, Av. Universidad 1001, Cuernavaca, Morelos, Mexico
[2]Facultad de Química-UNAM, Mexico
[3]Centro de Ciencias Físicas, UNAM Avenida Universidad s/n, Cuernavaca, Morelos, Mexico
[4]Esc. de Ciencias e Ingeniería de Materiales, U. Central de Venezuela, Caracas, Venezuela
[5]Instituto de Investigación de Materiales-UNAM, Mexico
[6]Materials Modification, Inc. Fairfax, VA, USA

*Corresponding author, email bci@fis.unam.mx

Published by Maney on behalf of the Institute
Received 3 June 2005; accepted 8 December 2005
DOI 10.1179/174329406X108843

substrates were carried out. The coated material was deposited under different parameters conditions with the PES technique. Relationships between the deposition parameters and the microstructural properties are explored.

Experimental

Pulsed electrode surfacing process

A 4 mm diameter sintered electrode of TiC with 2 wt-%Fe as a binder additive and additions of 2%B in order to increase the electrode ductility, was used for depositing coatings on AISI 8030, an alloy steel widely used for general engineering purposes. In the past[11,12] deposition employing PES technique has been conducted in lower carbon steels. By the PES technique, which is described in detail elsewhere.[11,12] Several steel coupons of $2{\cdot}54 \times 2{\cdot}54$ cm were polished by 240 grit emery paper and subsequently, cleaned in alcohol twice before deposition. The deposition was carried out using a hand held gun in air at room temperature. Two different operation modes of the PES process were used during deposition: the resistance–capacitance (RC) mode and the tyristor (TT) mode. All deposition parameters have been maintained constant and only three different modes of deposition were tested regarding the circuit employed. The first group of samples, identified as T1, has been obtained by a simple RC circuit with a current of 24 A. The second group of samples, identified as T2, has been produced by a TT mode with a current value of 2·2 A. The third group of coated samples, identified as T3, has been obtained by the TT mode and the RC mode with a current value of 6 and 10 A respectively. The spark time for all conditions was of 50 ms and their deposition conditions are summarised in Table 1. Past investigations[21] have shown that the RC mode produces a coating that rapidly increases in thickness and the coating surface is commonly very rough. However, for the layers obtained with the TT mode the coating thickness increases slowly and the obtained surface is smooth.

Structural and chemical characterisation

The microstructural and chemical characteristics of the coated layers were obtained using scanning electron microscope Jeol 6400 (SEM), transmission electron microscope Jeol 2010–200Kv (TEM) and X-ray diffraction techniques. Microstructural, morphological and chemical characterisations were obtained from the surfaces of the coated layers and also from the cross-section specimens, which include the interface between the coated layer and the substrate. The SEM specimens were initially prepared by mechanical polishing. They were washed in methanol using an ultrasonic bath. To reveal the microstructure the samples were etched with 2% nital. The chemical characteristics of the coating cross-sections were analysed with an energy dispersive X-ray (EDX) microanalysis system. The crystalline structural characteristics of the deposited coatings were obtained using an X-ray diffractometer with Cu K_α radiation ($\lambda = 1{\cdot}5406$ Å). X-ray diffraction patterns were unable to detect the presence of boron compounds perhaps, because the amount of these compounds in the coated layer is beyond the detection limit of this technique. Therefore, neutron diffraction technique was employed to explore the possible presence of TiB_2 in the coated layer. These experimental results were obtained using a neutron diffractometer coupled with a 1 MW Triga Mark III nuclear reactor ($\lambda = 1{\cdot}768$ Å). The samples for TEM observations were initially cut from the coated steel coupons. They were mechanically polished from both sides of the cut 3 mm diameter discs, leaving the coated layer from an initial thickness of 200 μm to a final thickness of 20 μm. Subsequently, the specimens were electropolished using a solution of 10% perchloric acid with ethanol at approximately -10°C.

Results and discussion

SEM experimental results

The topographical characteristics of the coated surfaces are illustrated in Fig. 1. It can be observed that all samples are characterised by an irregular surface roughness owing to the excessive globular mass transfer during the coating process from the electrode to the steel surface. Similar surface topographical characteristics have been obtained in other coated compounds using the same deposition technique.[11,12] In this case, the plasma formed has a high thermal conductivity that induces globular mass transfer,[22] then a molten globular droplet forms at the end of the electrode, which is accelerated by the plasma jet towards the steel surface, leading to a 'splash' appearance. The surface roughness was obtained in the same samples from a previous work[23] related to study the wear behaviour of these types of coatings. From these results, it can be pointed out that for the T3 samples a relatively smoother surface was obtained, which implied that a lower discontinuity in the coating formation was produced (Fig. 1*a*). Defects such as pores and cracks were observed. Pores are related to electrical characteristics and speed of traverse of the electrode. Cracks are due to the thermal expansion mismatch stresses created when the well bonded coating and the steel, are observed on top of

Table 1 Coatings characteristics

Sample	Processing conditions	Average coating thickness (region I), μm	Thickness of the heat affected zone (HAZ), μm	Knoop microhardness (region 1) HK_{100}	Knoop microhardness (region 2) HK_{100}	Knoop microhardness (HAZ) HK_{100}
T1	RC (24 A); 50 A pulse; 100 Hz pulse frequency	363·6±31·1	213·1±74·8	2026±343·9	568·2±138·9	201·8±27·1
T2	TT (2·2 A); 50 A pulse; 75 Hz pulse frequency	172·8±56·6	159·1±21·1	1828±274·15	565·1±64·1	319·6±48·7
T3	RC (10 A); TT (6 A); 50 A pulse; 50 Hz pulse frequency	106·2±17·9	74·5±24·7	1493·3±221·4	679·7±168·2	323·4±46·3

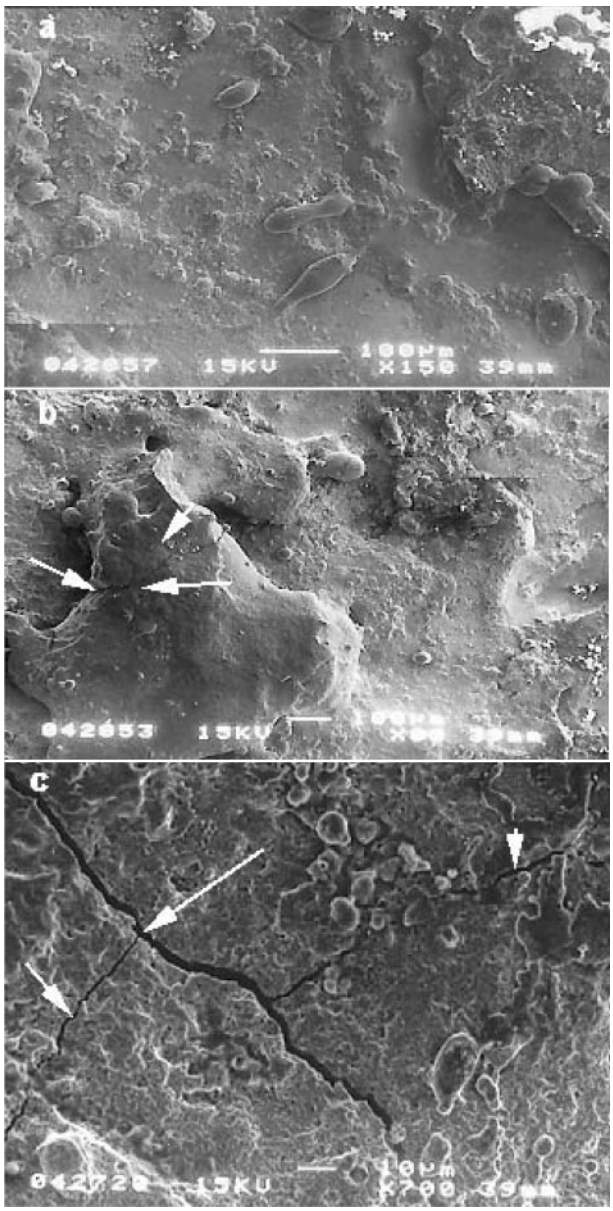

a T3 sample; *b* T2 sample; *c* T1 sample

1 Topographical characteristics of coated surfaces, SEM images obtained from surface of coated layers

the T1 and T2 samples (Fig. 1*b* and *c*). These cracks, as indicated by arrows in Fig. 1*c*, when observed on the cross-section of the coating, are perpendicular to the substrate surface owing to the fact that the well bonded coating is placed in tension when attempts to shrink, while the cooler substrate restricts such shrinkage.

Polished cross-sections were also observed with the SEM. The samples observed showed an adherent and continuous layer of ceramic coating on the steel substrate. However, the coating thickness is not uniform and in some places the area of uncovered substrate is higher. Measurements of the coatings mean thickness and the extent of the HAZ for all samples are also presented in Table 1. Sample T1 shows that both the coating thickness and the thickness of the HAZ are larger than for the other conditions. This indicates that in the former case, a higher heat input was applied.

Figure 2 shows as an example of the microstructural characteristics of the cross-section regions of sample T1. Three different regions could be distinguished: 1 – the coated layer, 2 – a small interface (HAZ) and 3 – the substrate. It can be observed a continuous interface and there is no the existence of cracks or delamination, this may indicate the formation of a metallurgical bond between the coating and the substrate. Analyses of the different regions from the cross-section samples were obtained by EDX. Typical X-ray compositional spectra from the different regions are illustrated in the inserts of Fig. 2. This spectrum shows the presence of Ti and C and traces of Fe in the coating. However, the interface is predominantly a mixture of Fe and Ti. The substrate consists basically of Fe and small amount of C. The high concentration of Ti within the coating and the interface is clearly shown (Fig. 2 regions 1 and 2), and also there is a high concentration of Fe in the interface which indicates that the formation of a metallurgical bond is due to the intermixing of the TiC and Fe. The mixing occurs at the deposit/substrate interface and the highly Fe concentration at this point is due to Fe from the substrate and from the binder used in the electrode material (2 wt-%). Also, it has been reported[24] that the high Fe concentration obtained is due to the large volume of molten Fe produced. Owing to the large difference in the melting points of the coating (in this case TiC) and the substrate (Fe), some of the precipitates, which contain Ti, have also been identified at the coated layer (region 1); these features are shown in detail by arrows in Fig. 3*a*. Also along the coated layer, it was also observed different regions which correspond to microstructural changes owing to the subsequent process (Fig. 3*b* and *c*). In Fig. 3*a*, the TiC particles are partially dissolved, which as shown Fig. 3*b* indicates a complete dissolution in the molten surface layer and reprecipitates as a dendritic microstructure during cooling. Similar microstructures produced by dispersion of TiC particulates in steel melt have been reported.[25] Figure 3*c* shows another microstructural change that occurred in the substrate (region 2) owing to an appreciable difference in local temperature during heating and subsequent cooling; a Widmastätten structure is formed.

Knoop microhardness measurements (HK_{100}) were conducted on the samples cross-sections in regions 1 and 2 and also on the substrate. The average values of Knoop microhardness shown in Table 1 do not show significant differences. However, comparing the average values of the coated samples region 1 (1782 280HK_{100}), there is an increase nearly one order of magnitude compared with the substrate value (163 11HK_{100}). Regarding region 2 the average value obtained was of 604 123·7 HK_{100}, which is almost four times greater than the corresponding microhardness value of the substrate. It has been reported similar microhardness values for martensite microstructures in medium carbon steels.[26] This may indicate that the microstructures obtained in regions 2 (Fig. 3*c*) can also be related to a martensite formation in the HAZ that is a consequence of the rapid heating and cooling rate attained during the process.

X-ray and neutron diffraction patterns results

The structural characteristics of the coated layers were obtained using X-ray and neutron diffraction techniques. The X-ray diffraction patterns obtained from the three samples are illustrated in Fig. 4. It is observed that the major peaks are identified as Fe and TiC phases;

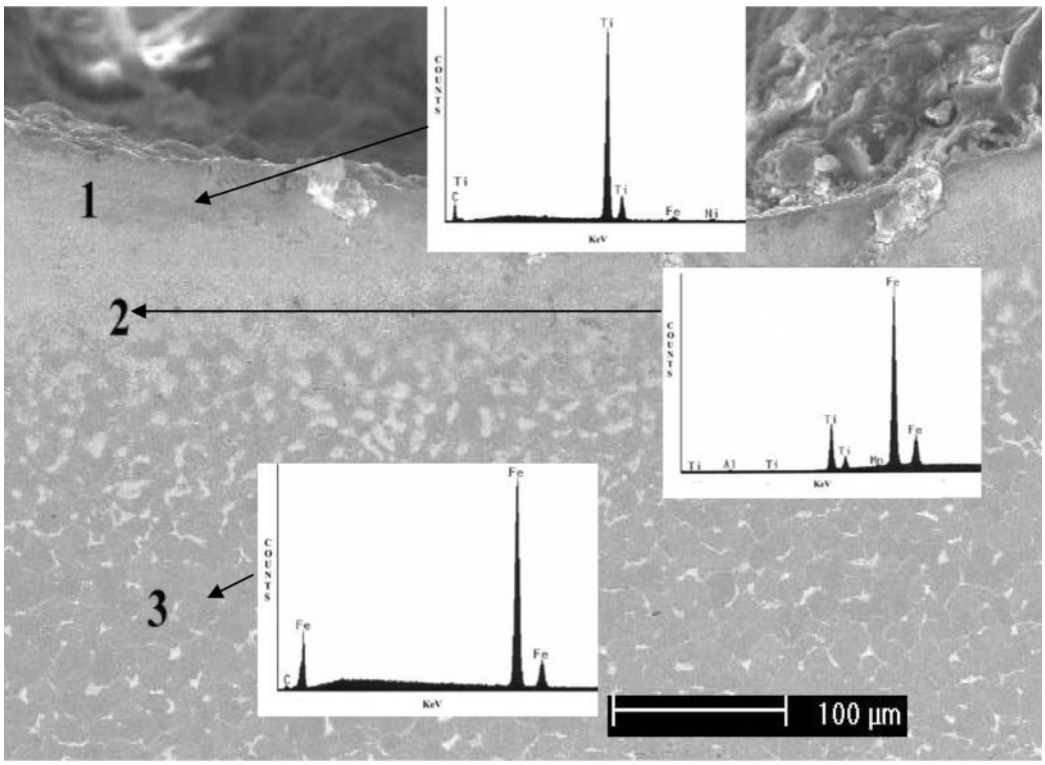

2 Image (SEM) showing examples of microstructural characteristics in cross-section regions of T1 sample: three different regions could be distinguished: 1 – coated layer, 2 – small interface (HAZ) and 3 – substrate; insert shows compositional EDX spectrums from different regions of sample

however there are several other peaks which may confirm the formation of metastable phases during the process. The presence of metastable phases is supported by the high energy density process such as PES. The highest amount of TiC in sample T1 indicates that for these samples a higher heat input was applied during processing which allows a higher degree of intermixing that occur between the molten substrate and the TiC electrodes. Although, when the process conditions are modified toward a lower heat input, a decrease in the TiC phase can be observed in T2 and T3 samples, however the differences between them are not considerable. The presence of Fe in the layer shown in Fig. 4, can be related to the wetting phenomenon shown by Ti based ceramics by Fe at high temperatures and also that Fe behaves as an excellent binder.[24,27,28] This suggests that Fe is present as a mixture into the TiC compound during the solidification of localised melt pool of TiC and Fe. As mentioned above, the higher Fe content is due to the significant difference between the melting points of the TiC coating and the Fe substrate. The Fe substrate has a lower melting point and forms a larger volume of molten material compared with the TiC electrode. Therefore the coating layer has a higher concentration of Fe.

Owing to its high free energy ($-319{\cdot}7$ kJ mol^{-1}) of formation ,[26] TiB_2 compound is also possible to be formed in the system. However, it was not detected

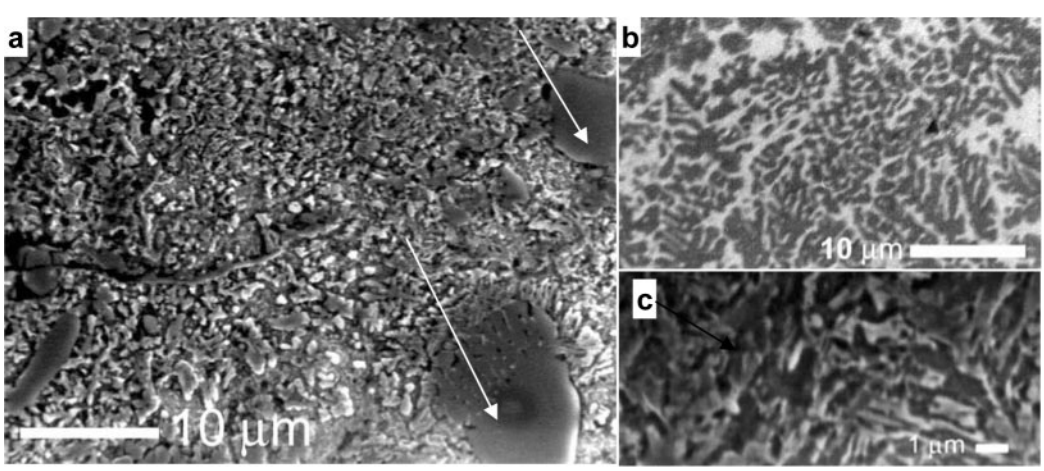

a TiC particles partially dissolved; *b* complete dissolution in molten surface layer and reprecipitates as dendritic microstructure during cooling; *c* another microstructural change that occurred in substrate (region 2) owing to appreciable difference in local temperature during heating, and subsequent cooling allowed the formation of Widmastätten structure

3 Different regions observed along coated layer which correspond to microstructural changes owing to subsequent process

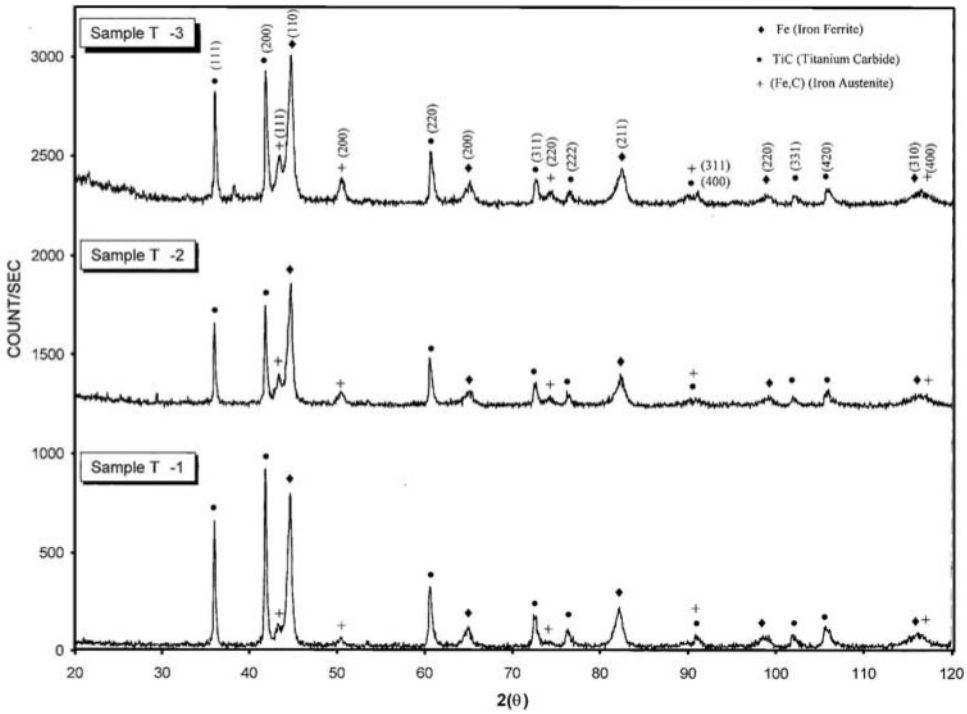

4 X-ray diffraction patterns for all coated samples: Fe and Ti carbide peaks can clearly be seen

through the X-ray analysis, the lack of detection of these types of compounds could be related with the small amounts of Boron used in the deposition process and also with the angular proximity of the TiB_2 diffracted peaks with TiC and Fe diffracted peaks. Neutron diffraction was employed as a complementary technique in order to avoid these difficulties and also to visualise the characteristic reactions that occurs during processing. Figure 5 shows a diffraction pattern obtained from sample T1, the indexation of this pattern confirms the presence of Fe and TiC in the coated layer and also small amounts of TiB_2 compound. This result confirms the nature of the PES process as a high energy density process[16,17] that leads to a rapid solidification of localised melt pools of TiC, Fe and B, and it could promote the formation of metastable phases.

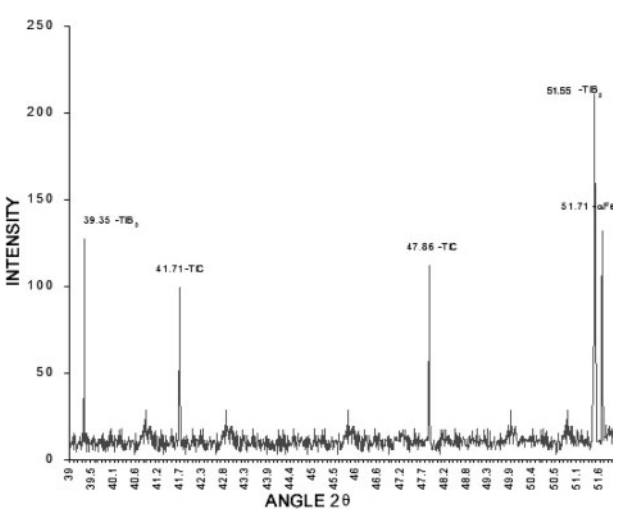

5 Sample T1 neutron diffraction pattern taken at coated layer: there are some diffraction peaks, which can be associated to TiB_2 compounds; these diffraction peaks were not resolved in X-ray diffraction patterns

TEM experimental results

Figure 6*a* and *b* shows a bright field (BF) image from the coated layer on the T1 sample. The figure illustrates the presence of precipitates of different sizes and also different morphological characteristics embedded in the Fe matrix. Two different types of precipitates can be observed. In one case (Fig. 6*a*), the average precipitate size is of the order of 35–50 nm, however, other particle

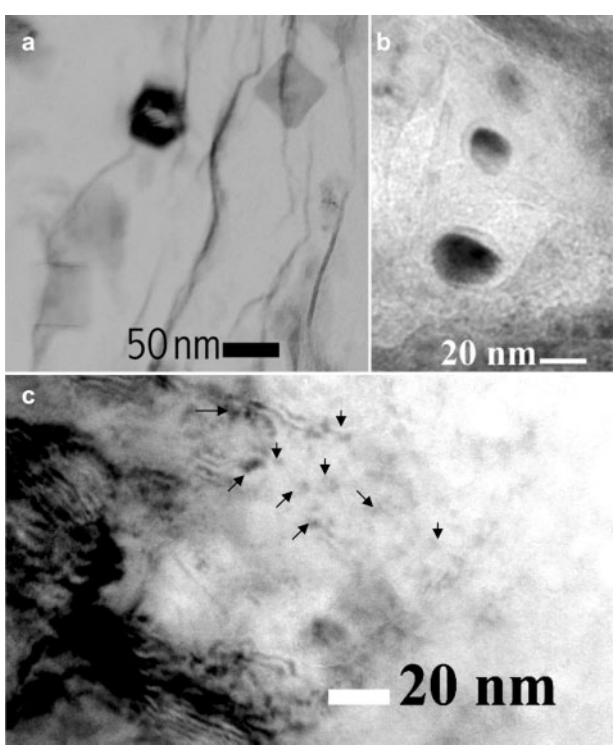

a 35–50 nm; *b* 10–20 nm; *c* another BF image

6 BF images from coated layer on T1 sample: size range of these precipitates is from 10 to 50 nm

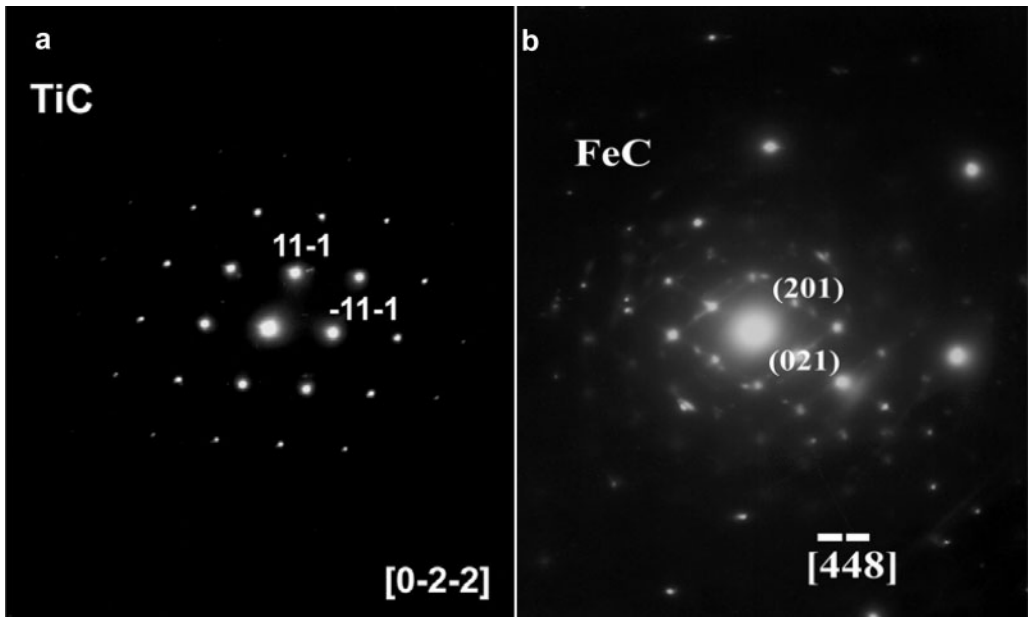

a TiC particles; *b* FeC particles

7 Typical diffractions patterns obtained from different particles from Fig. 6*c*

sizes are in the range of 10–20 nm (Fig. 6*b*). Also, several fine precipitates of nanometric scale were observed, but it was very difficult to isolate and characterise them. Figure 6*c* shows another BF image from the T1 specimen. This image shows contrast features of light and dark bands and also a high density of particles round and faceted indicated by arrows. These bands suggest different chemical compositions regions. Typical diffractions patterns obtained (Fig. 7*a* and *b*) from different particles from Fig. 6*c* indicate the presence of TiC and FeC particles. Their presence indicates that a higher heat input was applied during processing of the T1 samples, which in turn allowed a higher degree of mixing between the molten substrate and TiC, deposited from the electrode. Figure 8 shows TEM image of T2 sample. Particles of different morphologies can be seen randomly distributed in the Fe matrix. However, most of the precipitates have an apparent square or faceted shape, which implies that there is no preferred orientation between the particles and the matrix. The density of precipitates in these specimens is higher in comparison with the T1 case and also the average sizes are larger than in the T1 sample (20–60 nm). Figure 9 shows a BF image from the T3 sample. Precipitates with square or hexagonal shapes can be seen embedded in the ferritic matrix. The grain size in this case is $\sim$60 nm.

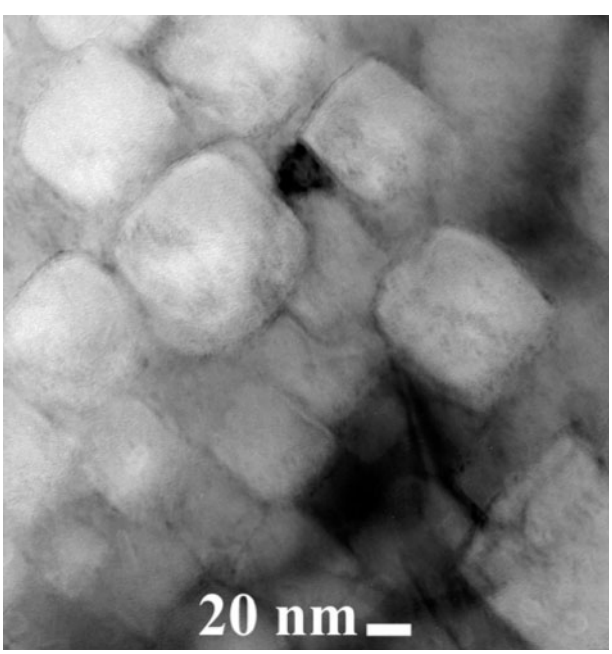

8 BF image (TEM) showing particles of T2 samples of different morphologies randomly distributed in Fe matrix

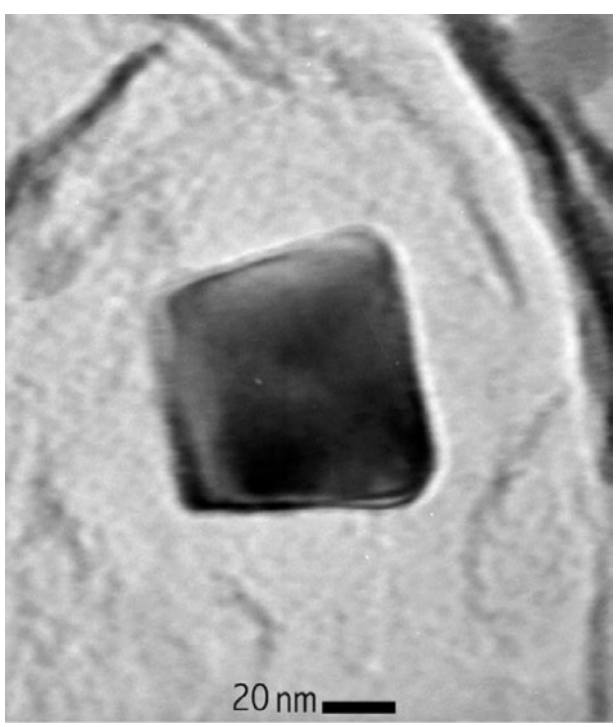

9 BF image (TEM) obtained from T3 sample

From the TEM results obtained, almost all the precipitates observed were composed mainly of TiC and FeC were randomly distributed in the Fe matrix, and also this was confirmed by microanalysis. This suggests that there is no preferred crystallographic orientation relationship between the particles and the Fe matrix. In addition, in some cases where the particles of TiC were in close contact the interface between the particles are uniform and does not exhibit any crack or delamination (*see* Fig. 8). This may indicate the strong bond between the TiC particles and the Fe matrix, and when particles are randomly distributed this behaviour is not perceptible. Also, the thermal expansion coefficient difference between the coated layer and the substrate is very small; this explains the absence of dislocations in the coating as it is observed in the bright field images. It is clear that in all processing conditions the morphology of the particles was polygonal and circular, similar shapes were obtained in TiB_2 coatings on Fe.[17] Although regarding their size and the chemical changes associated are due to different heat inputs during processing. This has been related[11] to an expression that involves the applied voltage and the amount of current and the duration of the current flow. In the present work, the voltage and the flow time used were kept constant, prevailing only the difference in the amount of current used as can be seen in Table 1. Therefore, for example, it can be observed that sample T1 has a higher deposition energy that gives rise to smaller particle sizes. On the other hand, when the deposition energy is lower, the particle size tends to increase.

Conclusions

TiC coatings have been successfully deposited on steel substrate using the PES technique. The coated layer is free of cracks and also forms a metallurgical bond with the substrate surface. Strong precipitation is obtained with different particle morphologies. Various size precipitates were associated with the processing conditions. Finer precipitates were produced under higher input energy conditions (T1 and T2 samples). A high density of precipitates ranging from 10 to 60 nm was shown. At lower input energy (T3 samples), the density of precipitates was lower and the sizes starts from 60 nm.

Acknowledgements

The authors would like to thank to NSF-Conacyt for economical support. The authors would like also to thank to R. Guardian, A. González and E. Herrera for the technical support.

References

1. C. F. Yen, C. S. Yust and G. W. Clark: 'New developments and applications in composites', 317–330; 1979, Warrendale, AIME.
2. N. B. Dahotre and S. Nayak: *Surf. Coat. Technol.*, 2005, **194**, 58–67.
3. A. J. Becker and J. H. Blanks: *Thin Solids Films*, 1984, **119**, 241–246.
4. J.-T. OK, I.-W. Park, J. J. Moore, M. C. Kang and K. H. Kim: *Surf. Coat. Technol.*, 2005, **200**, 1418–1423.
5. Y. T. Pei, D. Galvan, J. T. M. de Hosson and A. C. Nanostructured: *Surf. Coat. Technol.*, 2005, **198**, 44–50.
6. A. W. Mullendore, J. B. Whitley, H. O. Pierson and D. M. Mattox: *J. Vac. Sci. Technol.*, 1981, **18**, 1049–1053.
7. A. W. Mullendore, D. W. Mattox, J. B. Whitley and D. J. Sharp: *Thin Solid Films*, 1979, **63**, 243–249.
8. J. Chen and J. A. Barnar: *Mater. Sci. Eng. A*, 1995, **191A**, 233–238.
9. G. Hilz and H. Holleck: *Mater. Sci. Eng. A*, 1991, **139A**, 268.
10. A. Agarwal and N. B. Dahotre: *Int. J. Refract. Met. Hard Mater.*, 1999, **17**, 283–293.
11. A. Agarwal and N. B. Dahotre: *Mater. Character.*, 1999, **42**, (1), 31–44.
12. A. Agarwal and N. B. Dahotre: *J. Mater. Eng. Perform.* 1999, **8**, 479–486.
13. R. N. Johnson: in 'Surface modification technologies', (ed. T. S. Sudarshan and D. G. Bhat), 189–213; 1988, Warrendale, The Metallurgical Society.
14. E. A. Brown, G. L. Sheldon and A. E. Bayoumi: *Wear*, 1990, **138**, 137–151.
15. N. B. Dahotre, J. M. Hampkian and J. J. Stiglich in 'Elevated temperatures coatings: science and technology' (eds.): 303–312; 1995, Warrendale, PA, TMS.
16. N. Johnson: *Thin Solid Films*, 1984, **118**, 3411–3451.
17. A. Agarwal, N. B. Dahotre and L. F. Allard: *Prakt. Metall.*, 1999, **36**, (5), 250–263.
18. E. Kelesoglu and C. Mitterer: *Surf. Coat. Technol.*, 1998, **98**, 1483–1489.
19. J. R. Treglio, S. Trujillo and A. J. Perry: *Surf. Coat. Technol.*, 1993, **61**, 315–319.
20. J. Aromaa, H. Ronkainen, A. Mahiout, S. P. Hannula and E. Broszeit: *Mater. Sci. Eng. A*, 1991, **140A**, 722.
21. J. Stiglich, B. Campillo, I. Rosales and R. PÉREZ: *Surf. Eng.*, 1999, **15**, (4), 307–311.
22. R. N. Johnson: in 'Elevated temperatures science and technology I', (ed. N. B. Dahotre *et al.*), 264–277; 1995, Warrendale, PA, TMS.
23. M. H. Staia, A. Fragiel, M. Cruz, E. Carrasquero, B. Campillo, R. Perez, M. Constantino and T. S. Sudarshan: *Wear*, 2001, **251**, 1051–1060.
24. A. Agarwal and N. B. Dahotre: *Surf. Coat. Technol.*, 1998, **106**, 242–250.
25. T. Z. Kattamis and T. Suganuma: *Mater. Sci. Eng. A*, 1990, **128A**, 241–252.
26. G. V. Samsonov and I. M. Viniskii: 'Handbook of refractory compounds'; 1980, New York, IFI Plenum Data Company.
27. L. Ramquist: *Int. J. Powder Met.*, 1965, **4**, 1–4.
28. A. A. Ogwu and T. J. Davies: *Mater. Sci. Technol.*, 1993, **9**, 231–237.